5-2009

Extension of Gutenberg-Richter Distribution to Mw -1.3, No Lower Limit in Sight

Margaret S. Boettcher
University of New Hampshire, Durham, Margaret.Boettcher@unh.edu

Art McGarr
USGS

Malcolm J. Johnston
USGS

Recommended Citation

Boettcher, M. S., A. McGarr, and M. Johnston (2009), Extension of Gutenberg-Richter distribution to MW −1.3, no lower limit in sight, Geophys. Res. Lett., 36, L10307, doi:10.1029/2009GL038080.

Extension of Gutenberg-Richter distribution to M_W −1.3, no lower limit in sight

Margaret S. Boettcher,[1,2] A. McGarr,[1] and Malcolm Johnston[1]

[1] With twelve years of seismic data from TauTona Gold Mine, South Africa, we show that mining-induced earthquakes follow the Gutenberg-Richter relation with no scale break down to the completeness level of the catalog, at moment magnitude M_W −1.3. Events recorded during relatively quiet hours in 2006 indicate that catalog detection limitations, not earthquake source physics, controlled the previously reported minimum magnitude in this mine. Within the Natural Earthquake Laboratory in South African Mines (NELSAM) experiment's dense seismic array, earthquakes that exhibit shear failure at magnitudes as small as M_W −3.9 are observed, but we find no evidence that M_W −3.9 represents the minimum magnitude. In contrast to previous work, our results imply small nucleation zones and that earthquake processes in the mine can readily be scaled to those in either laboratory experiments or natural faults. **Citation:** Boettcher, M. S., A. McGarr, and M. Johnston (2009), Extension of Gutenberg-Richter distribution to M_W −1.3, no lower limit in sight, *Geophys. Res. Lett.*, *36*, L10307, doi:10.1029/2009GL038080.

1. Introduction

[2] At small magnitudes, several studies [*Aki*, 1987; *Iio*, 1991; *Richardson and Jordan*, 2002] have claimed evidence for a termination of the Gutenberg-Richter (GR) [*Gutenberg and Richter*, 1944] frequency-magnitude distribution (FMD), which can be expressed as $\log N(M) = a − b(M − M_C)$, where $N(M)$ is the cumulative number of events with magnitude greater than or equal to M, 10^a is the number of events above the catalog completeness M_C, and the slope b is typically near 1.0. Such studies address a long-standing controversy concerning the extent to which laboratory measurements can be applied to natural fault behavior. On the one hand, numerous reports [e.g., *Kanamori and Heaton*, 2000] suggest that the physics of rupture for major earthquakes differs from laboratory stick-slip friction, whereas, on the other hand, others [e.g., *Rice and Cocco*, 2007; *Scholz*, 1968] suggest that perhaps laboratory experiments can be directly applied to natural faults. An extension of the GR distribution to laboratory-scale stick-slip events would support the latter suggestion.

[3] A lower limit of FMDs also has implications for understanding earthquake hazard, both in terms of determining the size of the smallest earthquake that can trigger other earthquakes [e.g., *Sornette and Werner*, 2005] and the

size of the nucleation zone that may slip before an earthquake rupture becomes dynamic [e.g., *Dieterich*, 1992]. If slip in the nucleation zone is large enough, then it may be possible to detect it prior to an earthquake, at least in ideal situations, such as in deep mines, where monitoring instruments can be placed very close to earthquake sources. We therefore assess here the evidence for a minimum magnitude in TauTona Mine, South Africa, as proposed by *Richardson and Jordan* [2002].

2. Mining-Induced Seismic Catalog

[4] We analyze 285,007 earthquakes that were recorded between 1995 and 2006 in TauTona Mine. Integrated Seismic Systems International (ISSI) maintains the seismic network in the mine and manually processes the hundreds of $−2 \leq M_W \leq 4$ earthquakes recorded each day. At any time, approximately 20 stations operate in the depth range 1.8 km to 3.6 km. The standard network seismometers are geophones with a 4.5 Hz natural frequency; however, a variety of other sensors are occasionally used as well.

[5] Catalog data from a typical week are shown in Figure 1a, where the effect of the mine's daily blasting schedule is apparent. Ore production blasting occurs between 18:00–19:00 each weekday and on every other Saturday (F. Rheeder, personal communication, 2007), including Oct. 7, 2006. Stress changes associated with ore production enhance seismic activity during and directly following the blasting. No seismicity peak is observed on Sundays when the mine is closed. Figure 1a includes events located within 200 meters of the Carbon Leader Reef (CLR), which is an extensive, tabular, gold-bearing vein. Hypocenters of events within this distance of the CLR are mostly within the seismic network and therefore are the best located (typically have location errors of less than 40 m) and have the best-determined source parameters. In TauTona Mine the CLR is less than 0.1 m thick and is mined between 2.5–3.6 km depth (Figure 1b).

[6] Seismic moments in our earthquake catalog have been determined by ISSI using the spectral technique described by *Mendecki* [1997], based on *Aki and Richards* [1980]. Frequency spectra were calculated for all events with at least four identified phase picks at a minimum of four stations. The spectra were corrected for instrument response and stacked. The average displacement spectrum was corrected for attenuation and fit to Brune's model, $\Omega(f) = \Omega_0/[1 + (f/f_0)^2]$ [*Brune*, 1970], where Ω_0 is the long period amplitude of the displacement spectrum and f_0 is the corner frequency. Seismic moment was then calculated from Ω_0 as $M_0 = 4\pi\rho V_c^3 \Omega_0 R/\Re$, where ρ is the rock density, V_c is a constant wave speed set individually for each station, and $\Re$ is a root-mean square radiation pattern

---

[1]U.S. Geological Survey, Menlo Park, California, USA.
[2]Now at Department of Earth Sciences, University of New Hampshire, Durham, New Hampshire, USA.
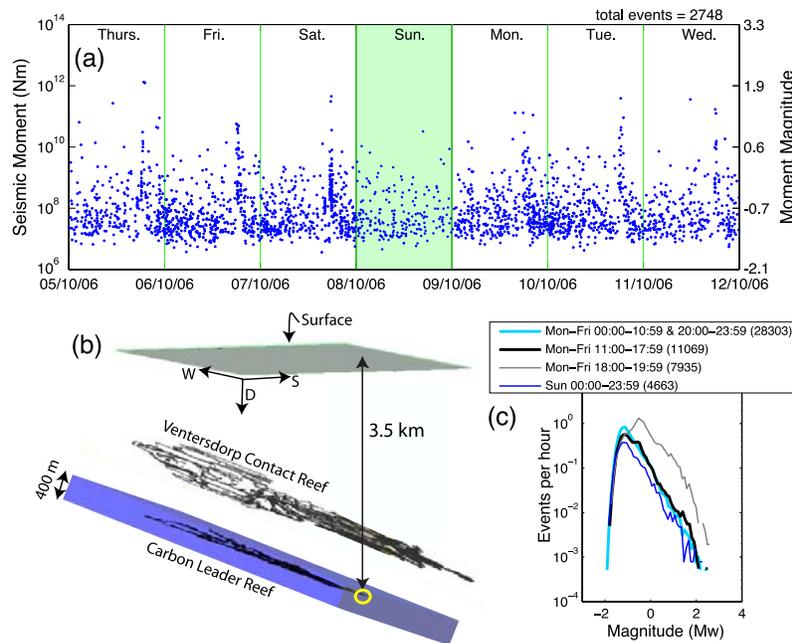
Figure 1. Seismicity recorded in 2006 in TauTona Mine. (a) Events from one week in October 2006 that occurred within 200 m of the CLR (inside the blue box in Figure 1b). (b) Actively mined regions of TauTona Mine. The blue box indicates the region used to select seismicity for our study. The yellow circle indicates the location of the NELSAM array. (c) Discrete FMDs of events within 200 m of the CLR from time periods associated with different levels of mining activity. The numbers in parenthesis in the legend refer to the total number of earthquakes in each FMD.

term, which is 0.55 for P and 0.63 for S. Moments were calculated individually for P, S_H, and S_V waves and then combined to determine a single estimate for the earthquake as $M_0 = [M_0^P + (M_0^{SH^2} + M_0^{SV^2})^{1/2}]/2$. M_0 was converted to M_W using *Hanks and Kanamori*'s [1979] relation, $M_W = 2/3(\log M_0 − 9.1)$.

[7] To verify the ISSI catalog M_0 values, we calculated moment tensors for 35 earthquakes using the technique of *McGarr* [1992] and compared scalar seismic moments determined from the deviatoric component of moment tensor to the catalog M_0 values. The deviatoric seismic

moments calculated in our moment tensor study [*Boettcher et al.*, 2008] range from 1.2×10^5 Nm to 4.7×10^{12} Nm. Over all, there is reasonable agreement between results for this small subgroup of events and those in the catalog. The few differences that we have identified, and are currently investigating, have no significant effect on the results presented here.

3. Populations of Mining-Induced Seismicity

[8] The evolution of the FMDs over time can be seen in Figure 2a. The unusual shape and curvature of the FMDs
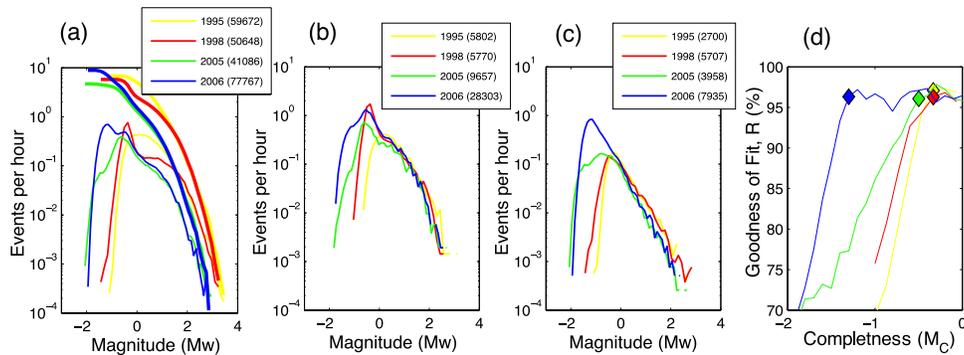

Figure 2. Frequency-magnitude distributions for seismicity recorded in TauTona Mine during 1995, 1998, 2005, and 2006. (a) Events recorded throughout the mine are included in the FMDs. Thick curves show cumulative distributions and thin curves show discrete distributions. (b and c) Discrete FMDs of events that occurred within 200 m of the CLR (b) during and immediately following blasting hours: Monday–Friday 18:00–19:59, and (c) during relatively quiet hours of working days: Monday–Friday 00:00–10:59 and 20:00–23:59. The total number of earthquakes in each FMD is given in parenthesis. (d) M_C values (diamonds) for the FMDs in Figure 2c at the magnitude at which 95% of the observed data are modeled by a straight line fit (see text for more details).

indicates that several types of earthquakes occur in TauTona Mine, consistent with observations from many previous authors who have investigated mining-induced earthquakes [*Gibowicz and Kijko*, 1994, and references therein; *McGarr*, 2005; *Richardson and Jordan*, 2002].

[9] With data from 1998 and 1999 in five South African gold mines, including TauTona Mine, *Richardson and Jordan* [2002] (hereinafter referred to as RJ) observed the same FMD as shown in Figure 2a (red curve). They noted the sharp inflection of the FMD at $M_W \approx 0$ and interpreted this as the approximate division between two populations of mining-induced seismicity, which they termed Type A and Type B events. RJ found that Type A events generally cluster in time (<30 s) and space (<100 m), have enriched high frequency source spectra, occur within 100 m of active mining, and have an upper magnitude cutoff at $M_{max}^{TypeA} \approx 1$. RJ associated Type A events with blasting, excavation, and stope closures. By contrast, Type B events were found to be spatially and temporally distributed throughout the mine and have FMDs that follow the GR distribution. RJ proposed that Type B events entail slip on pre-existing faults or fractures, perhaps analogous to tectonic earthquakes, but are limited to $M_{min}^{TypeB} \geq 0$, consistent with the inflection in the FMD (Figure 2a). Because Type A events were recorded at magnitudes lower than M_{min}^{TypeB}, RJ suggested that M_{min}^{TypeB} is a physical magnitude cutoff due to the nucleation zone size. Although we also find both Type A and Type B events in the mines, our conclusions, based on a larger catalog, differ from those of RJ in that we see no lower bound for Type B events.

[10] In this study, we separate earthquakes according to time of occurrence and distance from ore production, both of which strongly influence the catalog completeness M_C. Temporally, we separate populations by time of day (Figure 1) and year of occurrence (Figure 2). Careful scrutiny of Figure 1a shows fewer small earthquakes are recorded for two hours during and following production blasting. This deficiency of small events results from raising the trigger levels, which is done so that small events do not overwhelm the system during the several hours when seismicity rates are the highest.

[11] To obtain populations of seismicity with relatively uniform M_C, we separate earthquakes into four temporal groups based on the level of mining-related activity and recording trigger thresholds (Figure 1c). From low to high levels of activity, these groups include events recorded (1) on Sundays, when the mines are closed; (2) on working days during the low-activity hours, 00:00−10:59 and 20:00−23:59; (3) on working days during high-activity hours prior to ore production blasting, 11:00−17:59; and (4) during ore production and immediately following when the trigger levels are raised, 18:00−19:59. While the rate of $M_W > 0$ changed significantly between different time-of-day groups (Figure 1c), indicating that, on hourly time scales, the seismicity rate is tied to the level of mining activity, the rate of $M_W > 0$ showed almost no change for a time-of-day group over the 12 years (Figures 2b and 2c), suggesting that the overall rate of mining remained steady from year to year.

[12] Spatially, M_C increases quickly with distance from the network stations. To minimize changes in M_C, we limit our investigation to the best-recorded seismicity located within 200 m of the CLR (within the box in Figure 1b).

4. No Scale Break Above M_W −1.3

[13] Our simple separation procedure allows us to extract groups of mining-induced earthquakes that behave like tectonic earthquakes in that they follow a GR (power-law) distribution (Figure 2c) and consist primarily of Type B events, as defined by RJ's clustering criteria (further than 30 s and 100 m of another event). Because the parameters of the GR relation are sensitive to small variation in M_C, it is important to carefully determine M_C. To do so, we follow the procedure of *Wiemer and Wyss* [2000]. We use a maximum likelihood technique [*Aki*, 1965] to estimate the best-fit a and b values as functions of minimum magnitude M_i, for $M \geq M_i$ and then compute a synthetic distribution from the GR relation using the maximum likelihood values of b, a, and $M_C = M_i$. For each M_i we determine the absolute difference $R(a, b, M_i)$ between the cumulative number of events in each magnitude bin in the observed B_i and synthetic S_i distributions [*Wiemer and Wyss*, 2000], $R(a, b, M_i) = 100 - (100 \, (\sum_{M_i}^{M_{max}} |B_i - S_i|)/\sum_i B_i)$. M_C is determined to be at the point where the synthetic power law models 95% or more of the FMD (Figure 2d).

[14] The populations of earthquakes recorded within 200 m of the CLR during the lower-levels of mining activity (00:00−10:59 & 20:00−23:59 Mon.−Fri., and on Sundays) show GR distributions with b-values near 0.85 (Figures 1c and 2c). We compute M_C values for the curves in Figure 2c and obtain values of −0.3, −0.3, −0.5, and −1.3 for 1995, 1998, 2005 and 2006 respectively (Figure 2d). Using the maximum likelihood method for $M \geq M_C$, we compute b-values at the 95% confidence level: 0.85 ± 0.02, 0.76 ± 0.02, 0.90 ± 0.03, 0.84 ± 0.01 for 1995, 1998, 2005, and 2006. In each year, M_C is lowest on Sundays and the quiet times of the working days. $M_C = -1.3$ for both time periods in 2006 (Figure 1c). By separating events into groups according to the level of activity occurring in the mine, we find that M_C for the low-activity hours is significantly less than $M_{min}^{TypeB} = 0$ [*Richardson and Jordan*, 2002].

[15] Using RJ's clustering algorithm for separating Type A and Type B events, we find that 95% of the events in the low-activity hours can be classified as Type B events. Removing the 5% of Type A events does not change M_C or b. Data from 2006, when the seismic network capabilities and data storage capacity were best, show that the FMD of Type B events extends with no scale break to M_W −1.3, such that $M_{min}^{TypeB} = M_C$. Thus, our results indicate that the minimum magnitude for type B earthquakes proposed by RJ was due to detection limitations, not earthquake source physics.

5. Observations From NELSAM

[16] The above catalog analysis leads us to the question of whether or not M_W −1.3 could be the minimum magnitude in TauTona Mine for earthquakes that resemble tectonic earthquakes. To address this question we present
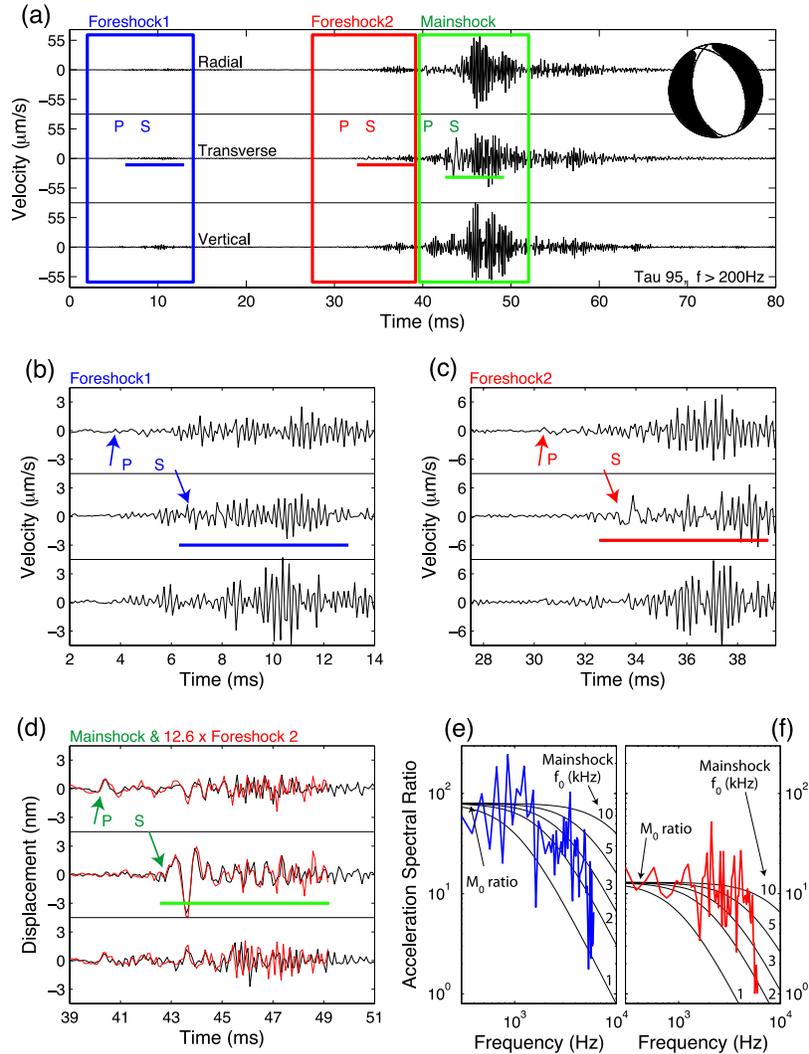
Figure 3. (a) Velocity records for three earthquakes recorded on station Tau95 at a distance of 27m at 10:08, Sept. 01, 2007. Body wave onsets are indicated for each event. Waveforms have been high-pass filtered above 200 Hz. The normal faulting mechanism was calculated for the mainshock. Horizontal lines indicate the portion of the waveform used to calculate the spectral ratios in Figures 3e and 3f. (b and c) Zoomed in records of the two foreshocks. (d) Mainshock (black) and foreshock 2 (red) filtered between 0.5 and 5 kHz and integrated to displacement. Foreshock 2 was multiplied by a factor of 12.6 and advanced by 9.9 ms to overlay the mainshock. Spectral ratios, calculated from the transverse component, between (e) the mainshock and foreshock 1 and (f) the mainshock and foreshock 2. The black curves in Figures 3e and 3f are model spectral ratios as described in the text.

initial observations from the Natural Earthquake Laboratory in South African Mines (NELSAM) project, which consists of a seismic network that spans 310 m laterally and 60 m vertically and is located near the deepest part of TauTona Mine (yellow circle in Figure 1b). The NELSAM seismic network includes five weak-motion, three-component accelerometers (±3g), three strong-motion, three-component accelerometers (±10g), and three three-component geophones. The NELSAM seismometers have been recording intermittently and thus have not yielded a comprehensive catalog. Nonetheless we have excellent examples of individual events.

[17] Some of our best-recorded small events include two foreshocks to a M_W −2.7 "mainshock", which occurred when the mine was closed for production on Saturday September 1, 2007 (Figure 3). The three earthquakes occurred within 50 milliseconds of each other and were recorded on four NELSAM seismometers, located at three sites at distances of 27 m, 70 m, and 169 m. We calculated a seismic moment tensor for the mainshock following the technique of *McGarr* [1992] and assuming a constant Q = 200. We determined a normal faulting mechanism with a scalar seismic moment of 1.2×10^5 Nm. We used the ratio of the waveform amplitudes to estimate the seismic moments of the foreshocks, which we found to be 1.5×10^3 Nm (M_W −3.9) and 9.5×10^3 Nm (M_W −3.4), for foreshock 1 and foreshock 2 respectively.

[18] The foreshock waveforms closely match those of the mainshock, as shown in Figure 3d, where the ground displacement from foreshock 2 is amplified by a factor of 12.6 and shifted by 9.9 ms, indicating the three events had almost the same focal mechanisms. The match between the

pulse widths of the two events in Figure 3d is due to the effects of attenuation and thus does not reflect the true pulse widths or corner frequencies of the earthquakes. To obtain an estimate f_0, we computed the acceleration spectral ratios between the mainshock and each of the foreshocks (Figures 3e and 3f), from the transverse component using the 0.0067 s following the S-wave onset (indicated by the horizontal lines in Figures 3a–3d). The record length was limited by the short time interval between foreshock 2 and the mainshock. Figures 3e and 3f display model curves (black lines) for the spectral ratios, which were calculated assuming all three events could be fit with *Brune*'s [1970] spectrum and a constant stress drop model, i.e. $M_0 \propto f_0^{1/3}$. We investigated a range of possible f_0 values for the mainshock, including 1, 2, 3, 5, and 10 kHz. The model curves in Figures 3e and 3f suggest that the mainshock corner frequency is between 2 and 5 kHz, which is consistent with an extrapolation of *Yamada et al.*'s [2007] results.

[19] To estimate earthquake source sizes, we use *Brune*'s [1970] model, $r = 2.34\beta/(2\pi f_0)$. For the mainshock, we determine $0.3 \leq r \leq 0.7$ m and, for the foreshocks, it appears that $f_0 > 3$ kHz, which implies $r < 0.5$ m. Furthermore, the nucleation zone size of these earthquakes must be smaller than ~ 0.5 m, and therefore well below the length scale proposed by RJ of ~ 20 m.

6. Conclusions

[20] If there is a lower limit to the Gutenberg-Richter relation for earthquakes in South African gold mines, then we have shown that it is demonstrably below the completeness of the catalog at M_W -1.3, with, as yet, no minimum magnitude in sight. The scale of our observations overlaps those of shear failure in acoustic emission laboratory experiments, which range from relatively large events [e.g., *Thompson et al.*, 2009] to those ~ 2.5 orders of magnitude smaller, approaching the grain scale [e.g., *Lei et al.*, 2000]. These observations imply that if there is a length-scale that constrains the smallest shear failure in the mines, then it must be small; less than the rupture length for the smallest shear failure seismic event. As the near source NELSAM seismic array continues to acquire data, we will hopefully be able to extend the Gutenberg-Richter FMD to smaller magnitudes. However, we suspect that even with our high quality seismic array and very short hypocentral distances, we will not find a true minimum magnitude, because such an event is likely to be of the order of the grain size.

References

Aki, K. (1965), Maximum likelihood estimate of b in the formula log N = a − bM and its confidence limits, *Bull. Earthquake Res. Inst. Tokyo Univ.*, *43*, 237–239.

Aki, K. (1987), Magnitude frequency relation for small earthquakes: A clue to the origin of f_{max} of large earthquakes, *J. Geophys. Res.*, *92*, 1349–1355.

Aki, K., and P. G. Richards (1980), *Quantitative Seismology*, W. H. Freeman, San Francisco, Calif.

Boettcher, M. S., et al. (2008), A broadband, wide dynamic range investigation of earthquakes in deep South African gold mines, *Seismol. Res. Lett.*, *79*, 311.

Brune, J. N. (1970), Tectonic stress and the spectra of seismic shear waves from earthquakes, *J. Geophys. Res.*, *75*, 4997–5009.

Dieterich, J. H. (1992), Earthquake nucleation on faults with rate- and state-dependent strength, *Tectonophysics*, *211*, 115–134.

Gibowicz, S. J., and A. Kijko (1994), *An Introduction to Mining Seismology*, 399 pp., Academic, San Diego, Calif.

Gutenberg, B., and C. F. Richter (1944), Frequency of earthquakes in California, *Bull. Seismol. Soc. Am.*, *34*, 164–176.

Hanks, T. C., and H. Kanamori (1979), Moment magnitude scale, *J. Geophys. Res.*, *84*, 2348–2350.

Iio, Y. (1991), Minimum size of earthquakes and minimum value of dynamic rupture velocity, *Tectonics*, *197*, 19–25.

Kanamori, H., and T. H. Heaton (2000), Microscopic and macroscopic physics of earthquakes, in *GeoComplexity and the Physics of Earthquakes, Geophys. Monogr. Ser.*, vol. 120, edited by J. B. Rundle, D. L. Turcotte, and W. Klein, pp. 147–183, AGU, Washington, D. C.

Lei, X., K. Kusunose, M. V. M. S. Rao, O. Nishizawa, and T. Satoh (2000), Quasi-static fault growth and cracking in homogeneous brittle rock under triaxial compression using acoustic emission monitoring, *J. Geophys. Res.*, *105*, 6127–6139.

McGarr, A. (1992), Moment tensors of ten witwatersrand mine tremors, *Pure Appl. Geophys.*, *139*, 781–800.

McGarr, A. (2005), Observations concerning diverse mechanisms for mining-induced earthquakes, in *Proceedings of the Sixth International Symposium on Rockburst and Seismicity in Mines*, edited by Y. Potvin and A. M. Hudyma, pp. 107–111, Aust. Cent. for Geomech., Perth, West. Aust., Australia.

Mendecki, A. J., (Ed.) (1997), *Seismic Monitoring in Mines*, Chapman and Hall, London.

Rice, J. R., and M. Cocco (2007), Seismic fault rheology and earthquake dynamics, in *Tectonic Faults: Agents of Change on a Dynamic Earth*, edited by M. R. Handy et al., pp. 99–137, MIT Press, Cambridge, Mass.

Richardson, E., and T. H. Jordan (2002), Seismicity in deep gold mines of South Africa: Implications for tectonic earthquakes, *Bull. Seismol. Soc. Am.*, *92*, 1766–1782.

Scholz, C. H. (1968), The frequency-magnitude relation of microfracturing in rock and its relation to earthquakes, *Bull. Seismol. Soc. Am.*, *58*, 399–415.

Sornette, D., and M. J. Werner (2005), Constraints on the size of the smallest triggering earthquake from the epidemic-type aftershock sequence model, Båth's law, and observed aftershock sequences, *J. Geophys. Res.*, *110*, B08304, doi:10.1029/2004JB003535.

Thompson, B. D., R. P. Young, and D. A. Lockner (2009), Premonitory acoustic emissions and stick-slip in natural and smooth-faulted Westerly granite, *J. Geophys. Res.*, *114*, B02205, doi:10.1029/2008JB005753.

Wiemer, S., and M. Wyss (2000), Minimum magnitude of completeness in earthquake catalogs: Examples from Alaska, the western United States, and Japan, *Bull. Seismol. Soc. Am.*, *90*, 859–869.

Yamada, T., J. J. Mori, S. Ide, R. E. Abercrombie, H. Kawakata, M. Nakatani, Y. Iio, and H. Ogasawara (2007), Stress drops and radiated seismic energies of microearthquakes in a South African gold mine, *J. Geophys. Res.*, *112*, B03305, doi:10.1029/2006JB004553.

———————

M. S. Boettcher, Department of Earth Sciences, University of New Hampshire, 24 Nesmith Hall, 131 Main Street, Durham, NH 03824, USA. (margaret.boettcher@unh.edu)

M. Johnston and A. McGarr, U.S. Geological Survey, MS 977, 345 Middlefield Road, Menlo Park, CA 94025, USA.